Accepted Manuscript

Dynamic model of lithium polymer battery – Load resistor method for electric parameters identification

Daniel Gandolfo, Alexandre Brandão, Daniel Patiño, Marcelo Molina

PII: S1743-9671(14)20249-2

DOI: 10.1016/j.joei.2014.10.004

Reference: JOEI 87

To appear in: *Journal of the Energy Institute*

Received Date: 29 July 2014

Revised Date: 17 October 2014

Accepted Date: 20 October 2014

Please cite this article as: D. Gandolfo, A. Brandão, D. Patiño, M. Molina, Dynamic model of lithium polymer battery – Load resistor method for electric parameters identification, Journal of the Energy Institute (2014), doi: 10.1016/j.joei.2014.10.004.

Dynamic Model of Lithium Polymer battery – Load resistor method for electric parameters identification

Daniel Gandolfo[a], Alexandre Brandão[b], Daniel Patiño[a], Marcelo Molina[c]

[a] *Instituto de Automática, Universidad Nacional de San Juan, Argentina*

[b] *Department of Electrical Engineering, Federal University of Viçosa, Brazil*

[c] *Instituto de Energía Eléctrica, Universidad Nacional de San Juan, Argentina*

Abstract— Maximum battery runtime and its transients behaviors are crucial in many applications. With accurate battery models in hand, circuit designers can evaluate the performance of its developments considering the influence of a finite source of energy which has a particular dynamics; as well as the energy storage systems can be optimized. First, this work describes a complete dynamic model of a lithium polymer battery. In the sequel a simple and novel procedure is used to obtain the electric parameters of adopted model with the advantage of using only one resistor to represent the battery load and a pc-connected multimeter. The methodology used to identify the parameters of the battery model is simple, clearly explained and can be applied to various types of batteries. Simulation and experimental results are presented and discussed, demonstrating the good performance of the proposed identification methodology.

Index Terms— Lithium polymer battery, State of charge (SOC), Open circuit voltage, Battery model, Electrical parameters.

* Corresponding author. Tel. +54-264-154114739. Email-addresses: dgandolfo@inaut.unsj.edu.ar (D.Gandolfo), alexandre.brandao@ufv.br (A.Brandao), dpatino@inaut.unsj.edu.ar (D. Patiño), mgmolina@iee.unsj.edu.ar (M.G.Molina)

1 INTRODUCTION

Batteries have been more and more pervasively used as the energy storage and power source for various electrical systems and devices, such as communication systems, electronic devices, renewable power systems, electric vehicles, etc. Although the popularity of portable electronics has propelled battery technologies, such as nickel cadmium (NiCd), nickel-metal hydride (NiMH), lithium-ion (Li-ion), and polymer Li-ion, those battery technologies cannot yet meet the progressive energy demands and size limitations of today's portable electronics [21],[22] and mobile robots[1],[2].

Many traditional designers of a lot of battery-powered devices tend to assume that the battery is ideal, that is, it would have a constant voltage throughout the discharge, and would also have a constant capacity for all discharge profiles, which is not always true.

Battery models are essential for any battery-powered system design that aims at extending the battery's expected life and in battery power management using energy optimization approaches [3]. On the other hand, some devices must be tested taking into account the fact that the electric voltage used is neither constant nor ideal.

In recent years, a number of researchers have begun to investigate the characteristics of battery sources and their impact on low-power circuit optimization techniques and power management strategies. Many battery models have been proposed in the literature and the respective parameters are identified by different methods. In [27] the Gauss-Hermite quadrature filter (GHQF) is introduced to estimate battery state of charge (*SOC*) based on a common electrical analogue battery model useful for real time applications. The authors in [28] propose an Unscented Kalman Filter (UKF) for 'online' estimation of the Lithium-Ion battery model parameters and the battery *SOC*, based on the updated model. All these techniques required not simple equations and add power consumption related to perform the necessary calculations [26].

Moreover, the procedure to identify the battery parameters is not entirely clear in the literature; e.g. in [7], the values of resistors and capacitors of the proposed model are estimated by fitting experimental points, but it is not clear how these points have been experimental obtained.

But the other hand Ari Hentunen *et.al.* [32] presents an analytical time-domain-based parameter identification method for Thevenin-equivalent circuit based lithium-ion battery models. In [33] online adaptive parameter identification for lithium-polymer battery cells is presented and an observer based on the updating model to estimate the SOC is proposed. The authors in [34] proposes an adaptive hybrid battery model-based high-fidelity state of charge (SOC) and state of health (SOH) estimation method for rechargeable multicell batteries, where hybrid battery model consists of an enhanced coulomb counting algorithm for SOC estimation and an electrical circuit battery model. In all this cases the parameters identification is well explained and the presented methods perform well, but many electronic equipments are needed to perform the proposed experiment (electronic loads, power analyzer, current sensor, battery testing system).

This paper describes a novel and simple test-procedure that can be used to derive electric parameters of a lithium-polymer battery model in order to identify the parameters with a good tradeoff between accuracy and complexity. The state of charge of the battery can be obtained online through simple equations as demonstrated hereinafter. The major contributions of this work is a simple and rapid method for identifying electrical parameters of the adopted battery model by using only one resistor, instead of an electronic load as used in the literature.

This work is organized as follows: Section 2 reviews the state of the art in battery models. Section 3 explains the battery model adopted, presenting its main advantages and highlighting the dynamics of interest. Section 4 describes a battery test system and experimental procedure used to identify the

parameters of the model adopted. Section 5 presents the simulations results comparing with experimental data. Finally, some concluding remarks are presented in section 6.

2 BACKGROUND

Battery is a dynamic and nonlinear system with many chemical reactions. Its internal characteristics and circuit parameters change according to the state of charge (SOC) and the operational temperature. To understand how the batteries work, some authors have proposed mathematical models to predict the battery behavior under several workload conditions. In [8], a closed form analytical expression to predict the remaining capacity of a lithium-ion battery is presented. Rakhmatov and Virudhula in [9] developed an analytical expression to estimate battery lifetime though various time-varying loads by taking into account the changes in the concentration of the electroactive species inside the battery. A nonchemical based partially linearized (in battery power) input–output battery model, initially developed for lead-acid batteries, was developed in [10]; then after tuning the parameter values, the model can be extended to different types of batteries such as lithium-ion, nickel-metal hydride and alkaline. In order to present a battery model from a systems and controls perspective, a novel compact form of existing electrochemical model from literature is introduced in [11].

On the other hand, many electrical models of batteries, from lead-acid to polymer Li-ion batteries, have been presented in the literature [7], [12]-[14]. Electrical models are more intuitive and easy to handle when they are used in circuit simulators and alongside application circuits. Almost all the propose models include different interconnection topologies of resistors, capacitors and inductors (e.g. Thevening, Impedance and runtime-based electrical battery models). Heuristically, more *RC* circuits provide a better modeling accuracy; however, some criterions must be enacted to demonstrate how much it is appropriate. Thus, in [17] a single *RC* circuit was used justifying that it offers a suitable trade-off between performance, complexity and usability. In contrast, three *RC* circuits have been used in [13].

By the other hand, a simple resistor-capacitor battery model is proposed in [18], where the modeling errors caused by the simple model are compensated by a sliding mode observer. Moreover, a single resistor is used by the authors in [19] and the thermal effect is considered to generate a holistic understanding of the battery. In the same context, taking into account high switching frequency applications, in [14] the authors have considered an inductance and two *RC* networks. This inductive component (insignificant at low frequency), has the property that the impedance increases in the high-frequency region.

In the battery, ohmic resistance is as a consequence of the finite conductivity of electrodes and separators, the concentration gradients of ionic species near to the electrodes and the limited reaction rates (kinetics) at the electrode surfaces. The capacitive effects arise from double-layer formation at the electrode/solution interface which includes capacitance due to purely electrical polarization and capacitance from diffusion limited space charges (pseudo-capacitance). Both capacitive effects influence the transient response of the battery, especially during high rate reaction. The magnitude of each effect depends on the particular battery chemistry and on the design parameters (such as geometry, pore structure and materials of electrodes, electrolytes and discharge rate).

Moreover, in order to evaluate the best battery discharge policy, many authors are interested in the charge movement during discharge and recovery, then different models have been used like ‘diffusion model’ and ‘Kinetic Battery model’ (KiBaM) [21]-[24]. The main disadvantage of these models is the absence of I-V information which is important for circuit simulation and optimization.

In order to obtain specifics dynamics captured by different models, some authors have proposed a mixed model of the battery as demonstrated in [25]. Furthermore, T. Kim and W. Qiao [16], have proposed a hybrid battery model, which takes the advantages of an electrical circuit battery model to accurately predict the dynamic circuit characteristics of the battery and an analytical battery model to capture the

nonlinear capacity effects for the accurate tracking and runtime prediction of the battery state of charge (SOC). In addition, it is important to note that many efforts are still being conducted to find ways to model the behavior of the batteries, taking into account different operating conditions. This is evident in the recent literature [5],[6],[31].

In any case, the study of the state of the art suggests that a good starting point for choosing a specific battery model is to predefine the particular type of application and under which conditions the battery will work (in other words, the dynamics to be excited).

3 THE BATTETY MODEL

In this work the model adopted is the hybrid one, which is based on a mix of the electrical circuit battery model and Kinetic battery model (KiBaM) [16]. This model was chosen due to its capability of capturing nonlinear capacity effects (such as the recovery effect and rate capacity effect) and its accurate battery SOC tracking and runtime prediction. Moreover it can accurately capture dynamic electrical circuit characteristics and nonlinear behaviors of batteries. Furthermore, the model is effective for modeling any electrochemical batteries. Fig.1 shows a general hybrid battery model scheme. The advantage of this hybrid model is the possibility to chose the dynamic of interest by separated ways; e.g. electrical battery model can be chosen to be simpler or more complex according to the accuracy required (one, two or three constants times provided by the respective RC networks, with or without battery lifetime estimation, and so on).

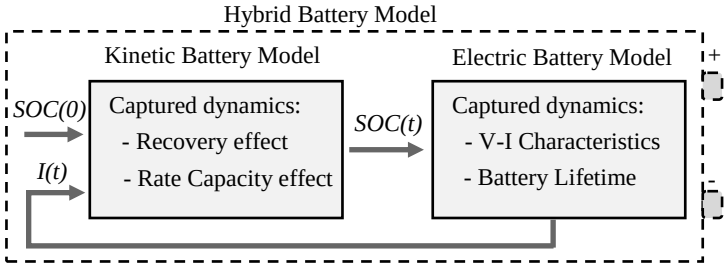

Figure 1. General hybrid battery model scheme.

3.1 KINETIC BATTERY MODEL (KIBAM)

The KiBaM can be understood as a two well model, comprising of an available charge well and a bound charge well. The available charge well supplies to the load directly while the bound charge well cannot do it so. However the bound charge well contributes in the replenishment ("Recovery Effect") of the available charge well. The charge transferred between the two wells is governed by the difference in their heights and their rate constant. A battery is said to be discharged when the available charge well becomes empty. The KiBaM describes the chemical processes of a battery by a kinetic process where concentration of the active species (charged ions of Lithium and Nickel) is uniform at electrode-electrolyte interface at zero current. As the intensity of the current is increased, the deviation of the concentration from the average becomes more significant and the state of charge as well as the cell voltage decrease. This phenomenon is called *Rate Capacity effect*. If cells in a battery are allowed to relax long enough after delivering electric current (e.g. pulse load), the diffusion process compensates for the depletion of the active materials that takes place during the current drain. The degree to which the battery recovers depends on the discharge profile (rate), the length and distribution of the idle slots and the battery design. This non-linearity in the battery has been termed the *Recovery effect*. The Kinetic battery model is capable to capture this nonlinear capacities effects (rate capacity effect and recovery effect) modeling the battery as two wells of charge where the charge is distributed with a capacity ratio c ($0 \leq c \leq 1$), as shown in Fig.2. The available-charge well supplies electrons directly to the load; the bound-charge well supplies electrons only to the available-charge well. The state of charge of the battery is h_1; e.g. when h_1 is unity the battery is fully charged and when it is zero the battery is fully discharged. The rate of charge that flow between the two wells is set by k and the difference in the heights of the two wells, h_1 and h_2. Note that parameter c corresponds to the fraction of total charge in the battery that is readily available.

Taking an example, a load *I* is drawn from the battery. The available-charge well would be reduced rapidly, and the difference in h_1 and h_2 would become large. Now, when the load *I* is removed, charge would flow from the bound-charge well to the available-charge well until h_1 and h_2 become equal again. The battery's open-circuit voltage would increase and now more charge would be available than it would have been if the load had been connected until h_1 went to zero. KiBaM is useful in getting an intuitive idea of how and why the recovery occurs.

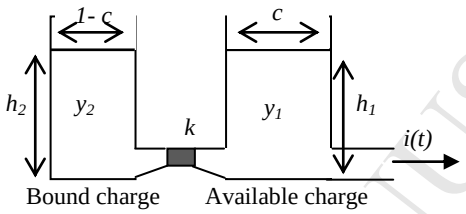

Figure 2. Kinetic battery Model (KiBaM).

The change of the charges in the two wells is expressed by the Eq.1 where y_1 and y_2 are the total charges in the available-charge well and the bound-charge well respectively; $h_1 = y_1/c$ and $h_2 = y_2/(1-c)$ and *i(t)* the load current.

$$\begin{cases} \dfrac{dy_1(t)}{dt} = -i(t) + k\left[h_2(t) - h_1(t)\right] \\ \dfrac{dy_2(t)}{dt} = -k\left[h_2(t) - h_1(t)\right] \end{cases} \tag{1}$$

The discharge completes when y_1 becomes zero, indicating a *SOC* equal to zero. Consequently, the unavailable charge *Cun(t)* of the battery can be expressed as follows:

$$\begin{aligned} Cun(t) &= (1-c)\,\delta(t) \\ \delta(t) &= h_2(t) - h_1(t) = \frac{y_2(t)}{(1-c)} - \frac{y_1(t)}{c} \end{aligned} \tag{2}$$

Where $\delta(t)$ is the height difference between the two wells, which plays an important role in obtaining the nonlinear capacity variation. Solving Eq.1 and Eq.2 and measuring the load current *i(t)*, the state of

charge of battery can be obtained using Eq.3 where *Cmax* represent the maximum capacity of the battery.

$$SOC(t) = SOC_{inicial} - \frac{1}{Cmax}\left[\int i(t)\,dt + Cun(t)\right] \quad (3)$$

Note that the recovery effect present in the battery and captured by this model unfailingly encourages thinking about the possibility of developing a battery discharge strategy that allows getting the highest possible autonomy.

3.2 ELECTRICAL CIRCUIT MODEL

Electrical models are more intuitive, useful, and easy to handle for Electrical engineers and their main advantage include the possibility of their application in circuit simulators. With this in mind and in order to obtain the Current-Voltage characteristic, two parallel *RC* networks and a single resistor have been adopted in this paper to describe the battery electrical model. The modeling error reduces drastically if two series connected RC parallel circuits are adopted. In contrast, if one RC parallel circuit is used to model a battery, non-ignorable modeling errors could exist [15].

In this work, the interest is to describe the discharge response of the battery during the time evolution of mission of a mobile robot. Therefore the battery lifetime estimation is not being taken to account in this work. Fig.3 shows the electrical circuit and the internal voltages drops, with the transient response being characterized by the *RC* networks. When a step load is apply to a battery, the instantaneous voltage drop is caused by resistor R_i and R_{TS}, C_{TS}, R_{TL}, R_{TL} are responsible for short- and long-time constant. A good tradeoff between accuracy and complexity can be obtained using two RC time constants, instead of one [17] or three [13]. Still observing Fig.3, V_{RC} is the total internal voltage drop. When an electric current is drained from the battery, V_{RC} subtracts the *Voc*.

However if no electrical current is required by the load, V_{RC} is added to *Voc*, and the voltage sum is reflected in *Vbat*.

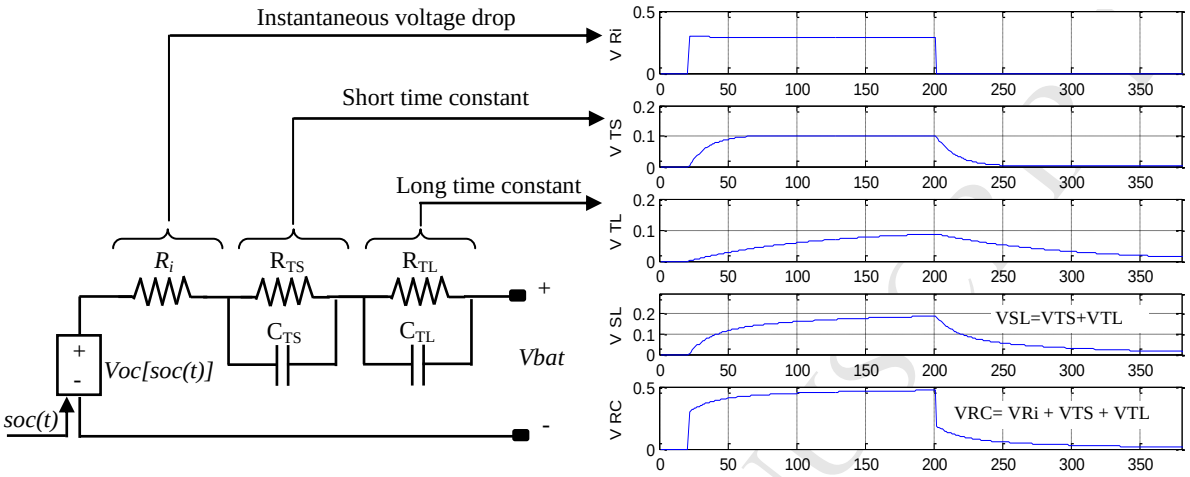

Figure 3. Electrical battery model and its internal voltages drop (instantaneous, short and long time constants).

This way, if a current *i(t)=I* is subtracted from the battery between time interval $t_0 \leq t \leq t_1$ and *i(t)=0* between $t_1 < t \leq t_2$ the system response is given by

$$
\begin{aligned}
&Vbat = Voc[SOC(t)] - V_{Ri} - V_{TS} - V_{TL} \\
&V_{Ri} = i(t)R_i \\
&t_0 \leq t \leq t_1 \Rightarrow \begin{cases} V_{TS} = R_{TS}\, i(t)\left[1 - e^{-(t-t_0)/(R_{TS}C_{TS})}\right] \\ V_{TL} = R_{TL}\, i(t)\left[1 - e^{-(t-t_0)/(R_{TL}C_{TL})}\right] \end{cases} \\
&t_1 < t \leq t_2 \Rightarrow \begin{cases} V_{TS} = V_{TS}(t_1)\left[e^{-(t-t_1)/(R_{TS}C_{TS})}\right] \\ V_{TL} = V_{TL}(t_1)\left[e^{-(t-t_1)/(R_{TL}C_{TL})}\right] \end{cases}
\end{aligned}
\tag{4}
$$

The relationship between *Voc* and *SOC(t)* is experimentally determined and explained in the next section.

4 EXPERIMENTAL SET UP AND PROCEDURE

It is widely known that all the parameters in the proposed model are multivariable functions of state of charge, current, temperature and recharge cycle number. These functions make the model extraction

complex (e.g., the fitting of multivariable functions or multidimensional lookup tables) and thus, the test process becomes too large. In order to minimize the system complexity, some subordinate parameters can be simplified (or even ignored) due they have negligible effects in polymer Li-ion batteries. Also, the usable capacity dependence on temperature is minimized due to the minor temperature fluctuations during low-power application and constant room temperature. The stronger dependence is related to the *SOC(t)*, hence the parameters are obtained as a function of this variable. This assumption not only simplifies identification process, but also provides a model with acceptable accuracy (good tradeoff). As aforementioned, the experiment is very simple and requires no complicated software or hardware tools. The test arrangement is shown in Fig.4.

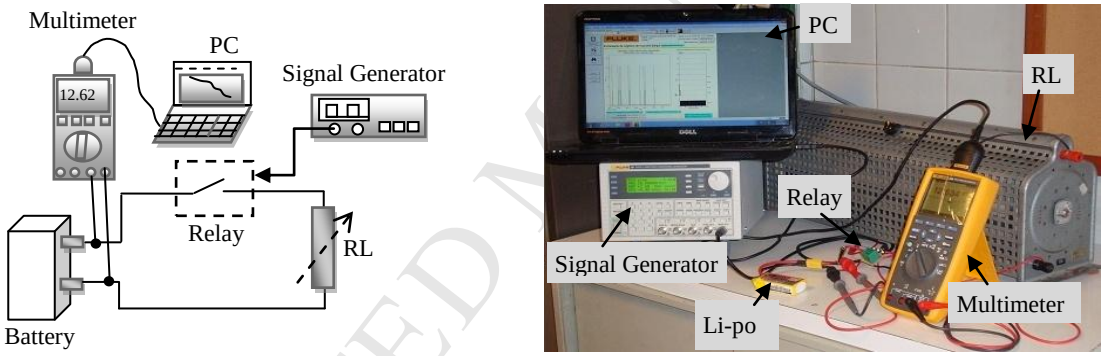

Figure 4. Schematic and real arrangement for testing battery.

The parameters of the used polymer lithium-ion battery used are listed as follows: Rhino 3S Lipoly Pack; nominal voltage: 11.1V; nominal capacity: 1050 mAh; discharge cutoff voltage Vcutoff: 10.5v (health condition); charge cutoff voltage Vover: 12.62v; and maximum discharge current: 20C (21A). The load used for the battery is R_L, which is an adjustable resistor (range of 1 to 20Ω and 220 watts). In order to avoid fluctuation in the ohmic value caused by heating, it is important that the load resistor has a current capacity much higher than the maximum current of the experiment.

Knowing that the experiment is performed at low frequency, a relay can be used as a switch element. The used relay has a contact resistant of 50 mΩ (0.05Ω) and this value is negligible compared to the value of load resistor and therefore is not taken into account in this experiment. However if another switching element is used with higher contact resistance or if the experiment is performed at higher load current, the voltage drop produced by the switching element must be considered. The switching frequency of the relay is guided by a signal generator though a square signal which allows discharging a battery with a pulse discharging current of different periods of time.

The log data of the experiment is obtained by using a Fluke 289 multimeter (mv resolution). The battery terminal voltage is sampled each 1 second and *FlukeView Form* software is used to logging the voltage values in a computer. The battery is charged at the same initial condition before each experiment, thus the initial open circuit voltage is 12.62v and the cut off voltage is 10.5v (3.5v per cell).

The battery is discharged at average c-rate of 0.9C (12Ω resistor) in portion of approximately 10% of state of charge, then approximately 6 minutes of rest period (rest period refer to the time with no load applied to battery) is taken into account and the terminal voltage is considered at the end of this time. If there is no load current, the voltage at the terminals of the battery represents the *Voc* when the transient response is extinct. While long-time constants of battery response are on the order of hours, the first 6 minutes give a enough information and makes the experiment practical and fast (non-extrapolated steady-state value of the best-fit exponential curve have been consider as occur in [30]). For the tested battery, between rest of period of 6 minutes and 1.3 hour, the terminal voltage varies only 0.04% after 2.2A of load current delivered, which does not justify the extra waiting time (the measures voltages are 12.388 in 6 minutes and 12.393v in 1.3 hour).

The maximum theoretical available charge of the battery is 3780A.s (1.05 Ampere * 3600 seconds), and then a 10 % of this charge represent 378A.s. Note that with a 12Ω as a load (R_L), the battery will deliver

an average current of 0.94A and will take approximately 380 seconds to deliver 10% of its maximum capacity. Then, the period of a square signal delivery by the generator is established at 760s (380 s ON and 380s OFF). The measured terminal voltage during the discharge process is shown in Fig.5 (left) together with a zoom when the battery has been discharged until the 80% of its capacity (right).

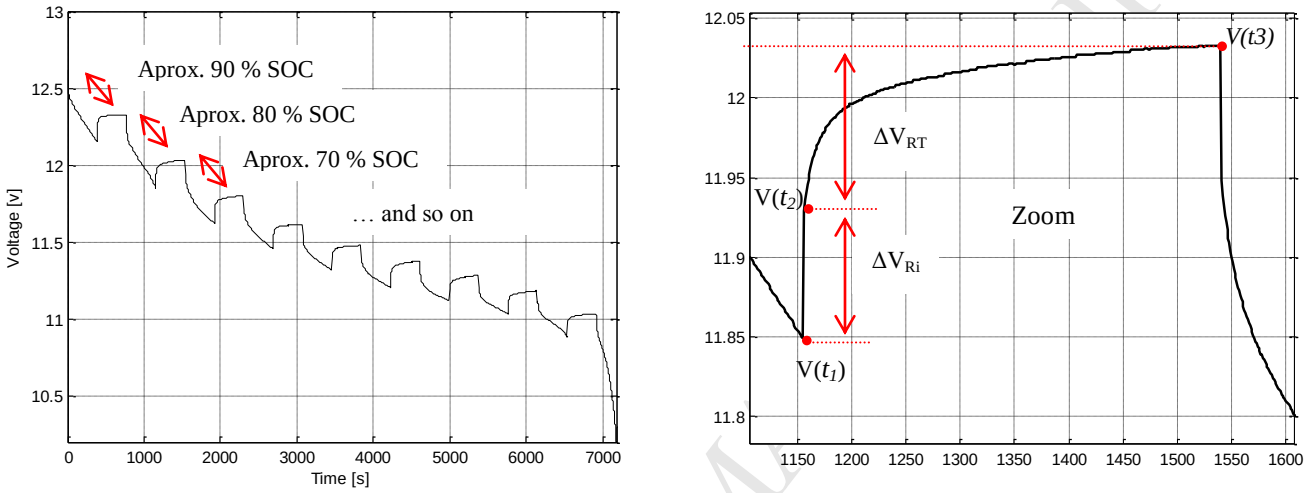

Figure 5. Battery terminal voltage measured during the discharge process and Zoom at 80% SOC

The challenge here is to estimate all the RC network parameters of the battery using only this measured data (*Vbat*). During the periods under load, the current delivered by the battery has been calculated as ($Vbat/R_L$). Thus the area under this calculated current represents the delivered Ampere-seconds, which are a portion of the total capacity of the battery. E.g, at the instant between 0 and 380s (ON period), the area under the current curve is 394.594A.s, which represent 10.439% of the total battery capacity (3780A.s). Hence the battery SOC at time t=380s is 100% - 10.439%=**89.561**% (100% correspond to battery fully charged at the beginning). Therefore the remaining state of charge of the battery after each period of delivery electric current has been experimentally extracted, resulting:

SOC = [100 ***89.561*** *79.389 69.488 59.74 50.098 40.635 31.202 21.816 12.547 6.434] %*

4.1 OPEN VOLTAGE ESTIMATION

In general, the battery open-circuit voltage (*Voc*) is a function of battery SOC and operating temperature [10]. Batteries are affected by environmental temperature. In this paper the experiment is performed at constant room temperature and normal environmental conditions are considered for the battery applications.

As aforementioned, the battery has been discharged approximately in portion of 10% of *SOC*, and the voltage at the end of each rest period has been considered. After that, the voltage *Voc=f [SOC(t)]* is estimated by using

$$Voc[SOC(t)] = a_1 e^{-a_2 soc} + a_3 soc^3 + a_4 soc^2 + a_5 soc + a_6 \quad (5)$$

to fit the points. The open circuit voltage as a function of state of charge is shown in Fig.6 where dots represent the last voltage value of the rest period (with no load, *Vbat=Voc*) and the continuous line is the fitted curve.

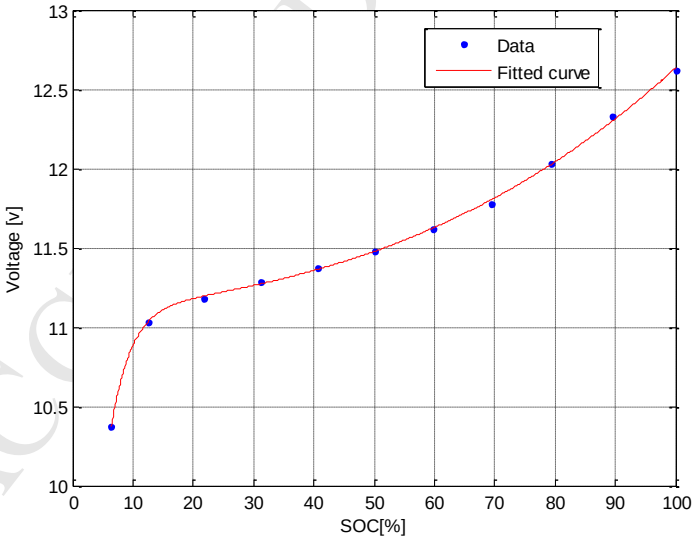

Figure 6. Battery open circuit voltage.

This nonlinear relation is very important to be included in the model (the best efforts must be done in a good approximation). In this paper, the parameters *c* and *k* used in the KiBaM for the proposed battery

were obtained in the same way as in [16]. The *c* parameter is obtained from Delivered capacity-Discharge current curve. In this case, *c=0.9187,* while *k=0.00017.* It is important to note that for another battery tested with similar characteristics (li-po 11.1v and 2200mAh) these parameters are also similar thus, these values are a good starting point to be used in new simulations. The charge in the battery is distributed with a capacity ratio *c* ($0 \leq c \leq 1$) and the initial conditions are: $y1(t0) = c \cdot \mathbf{C}$, $y2(t0) = (1-c) \cdot \mathbf{C}$ and $y0 = y1(t0) + y2(t0)$, where **C** is the total battery capacity. Then, in this case: $y1(t0) = 0.9187 \cdot \mathbf{C}$, $y2(t0) = (1-0.9187) \cdot \mathbf{C}$ and $\mathbf{C} = 1.050\text{A} \cdot 3600\text{s}$ (capacity in Ampere x seconds) . The charge value evolves according to Eq. (1) and SOC is calculated using (2) and (3). Later on, the voltage *Voc* can be obtained from (5).

4.2 RC NETWORK PARAMETERS ESTIMATION

Many papers take into account the identification parameters of the RC network for different topologies and most of them show the curves of each parameter as a function of *SOC.* However it is not always clear how these curves have been experimentally obtained, although equations that fit these curves are proposed. In a simple way, the method proposed here presents the advantage of requiring only simple resistor instead of an electronic load. Therefore this present work will help other researchers to make a simple, rapid and systematic identification of the battery model.

In the fig.5 ΔV_{Ri} represent the instantaneous voltage drop of the step response caused by R_i, and knowing the current value at time t_1 ($V_{(t1)}/R_L$), the resistor R_i can be calculated for each % of *SOC*. On the other hand ΔV_{RT} is the voltage drop caused by $R_{TS}+R_{TL}$ which has an associated constant time due the capacities C_{TS} and C_{TL}. Note that there are many parameters to be determined on the *RC* network and no enough information (just the measured terminal voltage of the battery). So a portion of curve shown in fig.5 between t_2 and t_3 is fitted in order to determinate the corresponding constants times. In the period time between t_2 and t_3 there is no load applied to battery, so this portion curve corresponds to a typical

resistive-capacity discharge (with a mixed short and long times constants) and it can be fitted by the Eq. (6) where τ_s and τ_L are the short and long time constant respectively.

$$V_{SL}(t) = \Delta V_{RT}\left[k_v\, e^{(-t/\tau_s)} + (1-k_v)e^{(-t/\tau_L)}\right]$$
$$where:\ \ \tau_s = R_{TS}\, C_{TS}\ \ ;\ \ \tau_L = R_{TL}\, C_{TL}\ ;\ 0 \le k_v \le 1 \qquad (6)$$

The fitting is done in Matlab program (nested 'for' loops algorithm) for each rest period, as is shown in Fig. 7 where the solid black line represent the real curve and red dotted line represents the curve adjusted. The constants times τ_s and τ_L are determined by the fitting for each period of no load conditions and have been showed in the graph. For simplicity, only the *% SOC* between 20-90 % has been plotted.

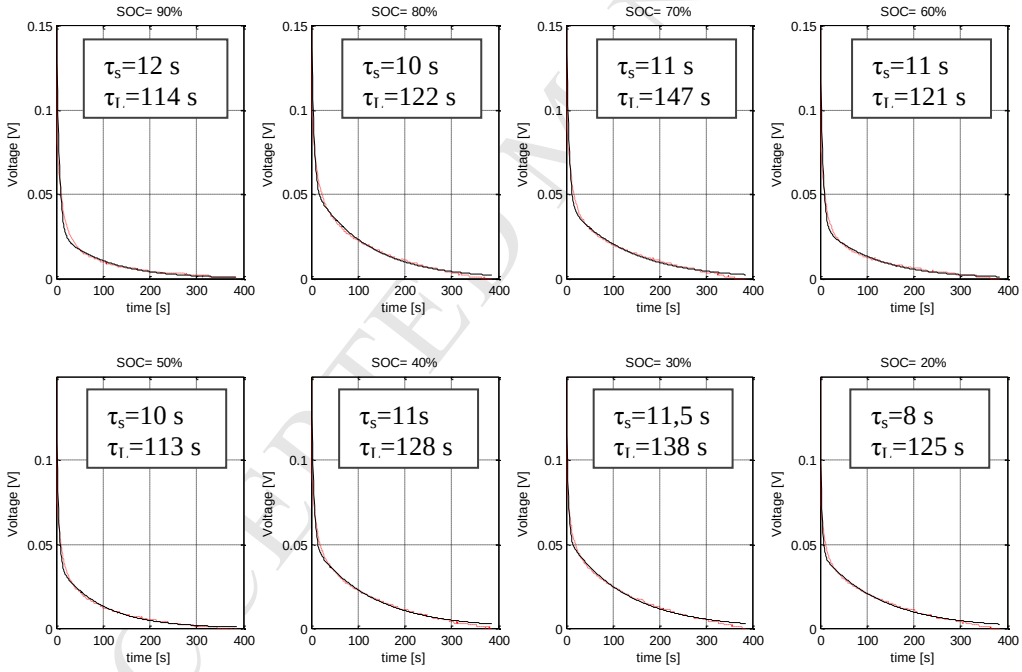

Figure 7. Voltage in R_{TS}+R_{TL} during rest period.

The parameter k_v is used just for fitting proposes and it represent the portions of voltage ΔV_{RT} applied in each parallel *RC* network individually. Since transient response depends on the calculated time constants and these are the product of *R* by *C*, it is valid to assume R_{TS}=R_{TL} and thus calculate the corresponding

capacitor value. The Eq. (7) are used for calculate all the parameters as function of *SOC(t)* each approximately 10% and after that, polynomials are used to fit the found points.

$$\begin{cases} R_i = \dfrac{\Delta V_{Ri}}{I} \Rightarrow R_i[SOC(t)] = \sum_{n=0}^{n=5} b_{(n)} \left[SOC(t)\right]^n \\ R_{TS} + R_{TL} = \dfrac{\Delta V_{RT}}{I} \Rightarrow R_{TS} = R_{TL} = \dfrac{\Delta V_{RT}}{2I} \\ R_{TS} = R_{TL} \Rightarrow R_{TSL}[SOC(t)] = \sum_{n=0}^{n=5} c_{(n)} \left[SOC(t)\right]^n \\ \tau_s = R_{TS}\, C_{TS} \Rightarrow C_{TS}[SOC(t)] = \sum_{n=0}^{n=5} d_{(n)} \left[SOC(t)\right]^n \\ \tau_L = R_{TL}\, C_{TL} \Rightarrow C_{TL}[SOC(t)] = \sum_{n=0}^{n=7} e_{(n)} \left[SOC(t)\right]^n \\ I = \dfrac{V(\mathrm{t}_1)}{R_L} \end{cases} \tag{7}$$

In Eq. (7), *I* represents instantaneous current at time t_1. For lithium polymer batteries this parameters are approximately constant over 20%–100% SOC and they change exponentially within 0%–20% SOC. Small parameter differences among the curves for different discharge currents indicate that these parameters are approximately independent of discharge currents and this can simplify the model since single-variable functions can be used to represent these curves [21]. Table.1 lists the coefficients of polynomials that fit the curves and figure 8 shows the curve of the electric parameters where the resistance values are expressed in ohm and capacity values in farads.

i	a_i	b_i	c_i	d_i	e_i
0	*-5.331*	*0.1381*	*0.1092*	*170*	*-0.0005e7*
1	*0.3053*	*-0.6113*	*-0.7727*	*-2115*	*0.0200e7*
2	*7.722e-007*	*2.4469*	*3.6710*	*16148*	*-0.1992e7*
3	*3.891e-005*	*-4.4802*	*-8.2696*	*-40267*	*0.9682e7*
4	*0.003777*	*3.8154*	*8.7117*	*42161*	*-2.5396e7*
5	*11.09*	-1.2281	-3.4389	-15922	3.6604e7
6					-2.7227e7
7					0.8154e7

Table 1. Parameters of fitted curves

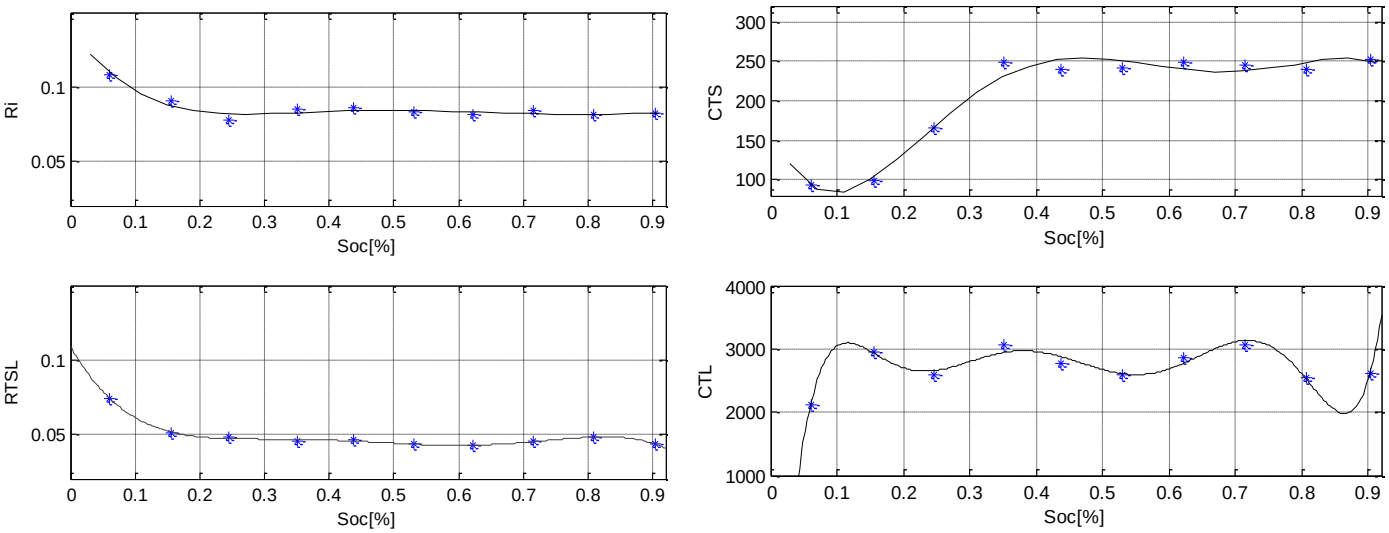

Figure 8. Electrical parameters of tested battery at room temperature.

5 MODEL VALIDATION

To validate the proposed method of parameter *extraction*, the Li-Po battery described in section 3 is tested with three different discharge profiles: Continuous discharge and Pulsed discharge with 120 and with 360 seconds of period (hereinafter *Ts*). In all of them, two loads value 12Ω (0.94A average current) and 5Ω (2.21A average current) are used. Fig. 9a shows the battery terminal voltage for continuous discharge considering average load current of 0.94A (0.9C) and 2.21A (2.2C). Fig. 9b and Fig.10a shows the battery voltage for the same load conditions but switched with a period of 120 seconds (60 seconds ON and 60 seconds OFF) and 360 seconds respectively (180 seconds ON and 180 seconds OFF). Finally Fig.10b shows the state of charge estimation for *2.2 C.*

The terminal voltage obtained from the proposed identification method match the experimental results in acceptable way. Therefore, the proposed model can accurately predict the runtimes of the battery under various discharge current conditions with an average error less than 0.6%.

If a better fit is needed, this same procedure can be performed considering e.g. discharge intervals of 5% of the SOC.

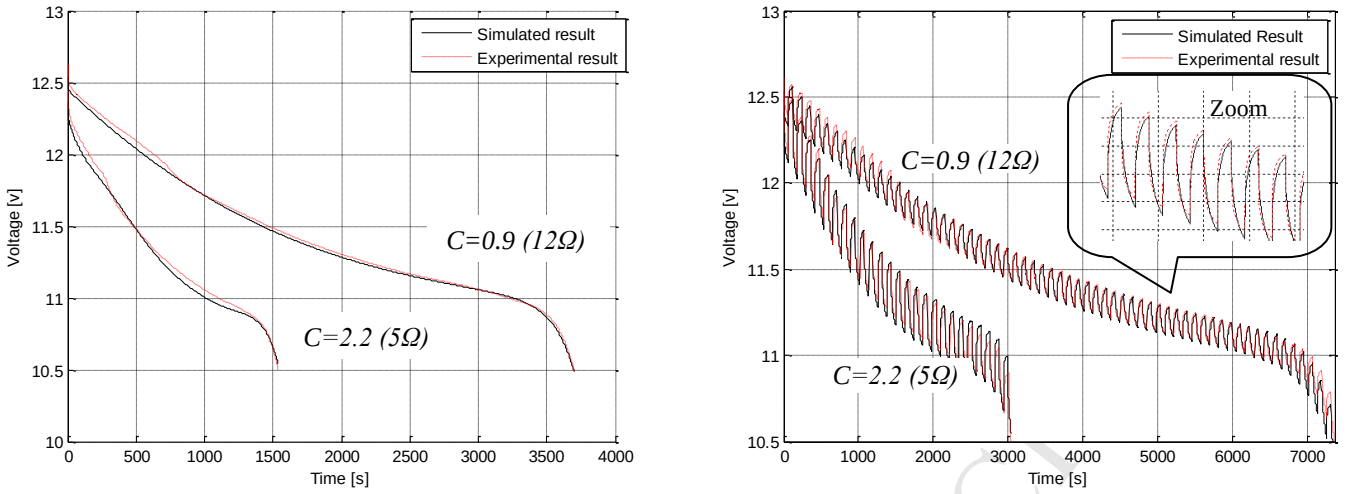

(a) (b)

Figure 9. Comparison of simulations and experimental results. (a) Continuous cases; (b) Switched case Ts=120 s

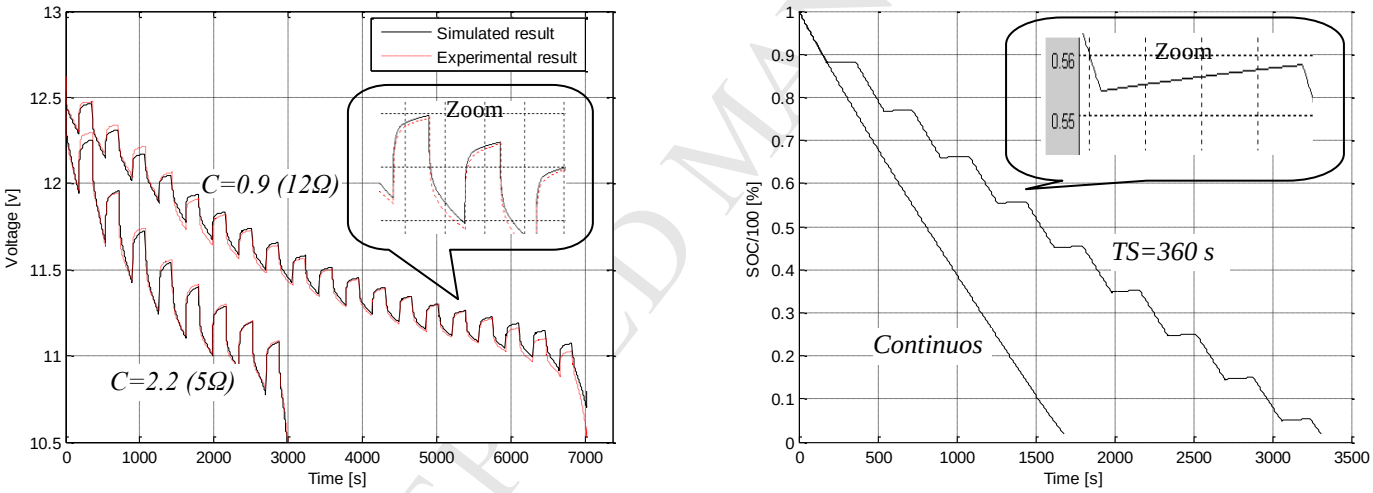

(a) (b)

Figure 10. (a) Comparison of simulations and experimental results for switched case Ts=360s; (b) SOC estimation.

But the other hand, Fig. 9 and 10 show that for an average c-rate of 2.2, the battery reaches the cut off voltage (10.5v) in 1530 seconds for continuous discharge, 3042s for Ts = 120s and 3000s for Ts = 360s. For an average c-rate of 0.9C, the time for continuous discharge is 3700s and 7370s for Ts = 360s. This indicates that the recovery effect is not significant on this battery because if it were, for the same c-rate,

the discharge time (time it takes the battery to reach the cutoff voltage) for switched case should be more than twice the continuous case (for equal ON and OFF times). The recovery effect can be seen in Fig. 10b (zoom), where it is observed that during periods without load, the SOC tends to rise rather than remain constant, but it does not happen significantly. These results agree with those obtained by L. Benini in [4].

6 CONCLUSION

This paper has examined the battery models found in the literature. A mixed model was adopted which takes the advantages of an electrical circuit battery model to accurately predicting the dynamic circuit characteristics of the battery and an analytical battery model to capturing the nonlinear capacity effects for the accurate SOC tracking and runtime prediction of the battery. A novel, rapid and simple test procedure was explained in order to identify the electric parameters of the model. Comparison of simulations results with experimental data shows an acceptable response indicating a good tradeoff between accuracy and complexity of the proposed method. On the other hand the incentives to think in a discharge policy of the battery based on exploiting the recovery effect are minimized; this is because the recovery effect in the tested battery did not had a magnitude of importance, as it was observed when comparing continuously and switched discharges.

ACKNOWLEDGMENTS

This work was funded by the Consejo Nacional de Investigaciones Científicas y Técnicas (CONICET – National Council for Scientific Research), and the Universidad Nacional de San Juan (UNSJ), Argentina.

REFERENCES

[1] C. Zhang and J.Kovacs, "The application of small unmanned aerial systems for precision agriculture: a review," An International Journal on Advances in Precision Agriculture, pp.693-712, 2012.

[2] J. Primicerio, S. Di Gennaro, E. Fiorillo, L. Genesio, E. Lugato, A. Matese y F.Vaccari, "A flexible unmanned aerial vehicle for precision agriculture," Technical Note, An International Journal on Advances in Precision Agriculture, Springer Science Business Media, 2012.

[3] R. Dougal, S. Liu and E.White, "Power and Life Extension of Battery–Ultracapacitor Hybrids," IEEE Transactions on components and packaging technologies, Vol. 25, no. 1, March 2002

[4] L. Benini, G. Castelliz, A. Maciiz, E. Maciiz, M. Poncino and R. Scarsi, "Extending Lifetime of Portable Systems by Battery Scheduling," in: Proceedings of the conference on Design, automation and test in Europe, IEEE Press Piscataway, NJ, USA, 2001.

[5] S. Han, S. Han and H. Aki, "A practical battery wear model for electric vehicle charging applications, Applied Energy," Vol.113, pp. 1100-1108, January 2014.

[6] L. Zhong, C. Zhang, Y. He and Z. Chen, "A method for the estimation of the battery pack state of charge based on in-pack cells uniformity analysis," Applied Energy, Vol.113, pp. 558-564, January 2014.

[7] M. Chen and G. Rincón-Mora, "Accurate Electrical Battery Model Capable of Predicting Runtime and I-V Performance," IEEE Transaction on Energy Conversion, vol. 21, no. 2, pp. 504–511. June 2006.

[8] P. Rong and M. Pedram, "An Analytical Model for Predicting the Remaining Battery Capacity of Lithium-Ion Batteries," IEEE Transaction on Very Large Scale Integration (VLSI), vol. 14, no. 5, pp. 441–451. May 2006.

[9] D. N. Rakhmatov and S. Vrudhula, "An analytical high-level battery model for use in energy management of portable electronic systems," IEEE/ACM International Conference Computer-Aided Design, 2001, pp. 488–493.

[10] V. Agarwal, K. Uthaichana, R. A. DeCarlo and L. Tsoukalas, "Development and Validation of a Battery Model Useful for Discharging and Charging Power Control and Lifetime Estimation," IEEE Transactions on Energy Conversion, vol. 25, no. 3, pp. 821–835. September 2010.

[11] N. A. Chaturvedi, R. Klein, J. Christensen, J. Ahmed and A. Kojic, "Modeling, estimation, and control challenges for lithium-ion batteries," in: American Control Conference Marriott Waterfront, Baltimore, MD, USA. June 30-July 02, 2010.

[12] L. Gao, S. Liu and R. A. Dougal, "Dynamic Lithium-Ion Battery Model for System Simulation," IEEE Transactions on Components and Packaging Technologies, vol. 25, no. 3, pp. 495–505. September 2002.

[13] R. C. Kroeze and P. T. Krein, "Electrical Battery Model for Use in Dynamic Electric Vehicle Simulations," in: Power Electronics Specialists Conference (PESC, IEEE). Rodhes, Greece, pp. 1336–1342. 15-19 June 2008.

[14] J. Jang and J. Yoo, "Equivalent Circuit Evaluation Method of Lithium Polymer Battery Using Bode Plot and Numerical Analysis," IEEE Transactions on Energy Conversion, vol. 26, no. 1, pp. 290–298. March 2011.

[15] H. Zhang and M.Y. Chow, "Comprehensive Dynamic Battery Modeling for PHEV Applications," in: Power and Energy Society General Meeting, IEEE, Minneapolis, pp. 1–6, 25-29 July 2010.

[16] T. Kim and W. Qiao, "A Hybrid Battery Model Capable of Capturing Dynamic Circuit Characteristics and Nonlinear Capacity Effects," IEEE Transactions on Energy Conversion, vol. 26, no. 4, pp. 1172–1180. December 2011.

[17] M. Einhorn, V. F. Conte, C. Kral, J. and R. Permann, "Parameterization of an Electrical Battery Model for Dynamic System Simulation in Electric Vehicles," in: Vehicle Power and Propulsion Conference (VPPC), IEEE, 2010.

[18] I. S. Kim, "Nonlinear State of Charge Estimator for Hybrid Electric Vehicle Battery," IEEE Transactions on Power Electronics, vol. 23, no. 4, pp. 2027–2034. July 2008.

[19] Y. K. Tan, J. C. Mao and K. J. Tseng, "Modelling of Battery Temperature Effect on Electrical Characteristics of Li-ion Battery in Hybrid Electric Vehicle," in: Ninth International Conference on Power Electronics and Drive Systems (PEDS), IEEE, Singapore, 5-8 December, 2011.

[20] M. Bernard, K. Kondak, N. Meyer, Y. Zhang, G. Hommel, "Elaborated Modeling and Control for an Autonomous Quad-rotor," in: 21st Bristol UAV Systems Conference, April 2007.

[21] V. Rao, N. Navet and G. Singhal, "Battery Aware Dynamic Scheduling For Periodic Task Graphs," in: 20th International Symposium in Parallel and Distributed Processing, IPDPS, Rhodes Island, 25-29 April, 2006.

[22] V. Rao, G. Singhal, A. Kumar and N. Navet, "Battery Model for Embedded Systems," in: 18th International Conference on VLSI Design, India, 3-7 January, 2005.

[23] T. Wang and C. G. Cassandras, "Optimal Control of Multi-battery Energy-aware Systems," in: 50th IEEE Conference on Decision and Control and European Control Conference (CDC-ECC), Orlando, FL, USA, December 12-15, 2011.

[24] T. Wang and C. G. Cassandras, "Optimal Discharge and Recharge Control of Battery-powered Energy-aware Systems," 49th IEEE Conference on Decision and Control, Atlanta, GA, USA, December 15-17, 2010.

[25] C. Antaloae, J. Marco and F. Assadian, "A Novel Method for the Parameterization of a Li-Ion Cell Model for EV/HEV Control Applications," IEEE Transactions on Vehicular Technology, vol. 61, no. 9, pp. 3881–3892. November 2012.

[26] O. Spinka and Z. Hanzálek, "Energy-Aware Navigation and Guidance Algorithms for Unmanned Aerial Vehicles," in: 17th IEEE International Conference on Embedded and Real-Time Computing Systems and Applications, 2011

[27] J. Lia, B. Jiab, M. Mazzolaa and M. Xinb, "On-line Battery State of Charge Estimation using Gauss-Hermite Quadrature Filter," in: 17th International Conference on Embedded and Real-Time Computing Systems and Applications (RTCSA), 2011.

[28] M. Partovibakhsh and G. Liu, "Online Estimation of Model Parameters and State-of-Charge of Lithium-Ion Battery Using Unscented Kalman Filter," in: American Control Conference, Montréal, Canada, June 27-June 29, 2012

[29] M. Coleman, W. G. Hurley and C. K. Lee, "An Improved Battery Characterization Method Using a Two-Pulse Load Test," IEEE Transactions on Energy Conversion, vol. 23, no. 2, pp. 708–713. June 2008.

[30] S. Abu-Sharkh and D. Doerffel, "Rapid test and non-linear model characterisation of solid-state lithium-ion batteries," Journal of Power Source, vol. 130, Issues 1-2, pp. 266–274. May 2004.

[31] R. Xiong, F. Sun, X. Gong and C. Gao, "A data-driven based adaptive state of charge estimator of lithium-ion polymer battery used in electric vehicles," Applied Energy, Vol. 113, pp. 1421-1433 January 2014.

[32] A. Hentunen, T. Lehmuspelto and J. Suomela "Time-Domain Parameter Extraction Method for Thévenin-Equivalent Circuit Battery Models," IEEE Transactions on Energy Conversion, Vol.29, no.3, pp.558-566, September 2014.

[33] H. Rahimi-Eichi, F. Baronti and MY. Chow, "Online Adaptive Parameter Identification and State-of-Charge Coestimation for Lithium-Polymer battery Cells," IEEE Transaction on industrial Electronics, Vol.61, no.4, pp. 2053-2051, April 2014.

[34] T. Kim, W. Qiao and L. Qu, "Online SOC and SOH Estimation for Multicell Lithium-ion Batteries Based on an Adaptive Hybrid Battery Model and Sliding-Mode Observer", IEEE Energy Conversion Congress and Exposition, Denver, U.S.A, September 2013.

HIGHLIGHTS

This paper describes a novel and simple test-procedure that can be used to derive electric parameters of a lithium-polymer battery model in order to identify the parameters with a good tradeoff between accuracy and complexity. The major contributions of this work is a simple and rapid method for identifying electrical parameters of the adopted battery model by using only one resistor, instead of an electronic load as used in the literature.